



Remarkable influence of reductant structure on the activity of alumina-supported silver catalyst for the selective catalytic reduction of NO_x

Yunbo Yu, Xiaoping Song, Hong He^{*}

State Key Laboratory of Environmental Chemistry and Ecotoxicology, Research Center for Eco-Environmental Sciences, Chinese Academy of Sciences, 18 Shuangqing Road, Haidian District, Beijing 100085, China

ARTICLE INFO

Article history:

Received 3 December 2009

Revised 27 January 2010

Accepted 14 February 2010

Available online 29 March 2010

Keywords:

Selective catalytic reduction

Alcohol isomer

Enolic species

α -H

Alumina-supported silver catalyst

ABSTRACT

This study investigated the selective catalytic reduction of NO_x over alumina-supported silver catalyst by butyl alcohol isomers. Butyl alcohol (BA), sec-butyl alcohol (SBA), and isobutyl alcohol (IBA) showed similarly high efficiency for NO_x reduction at low temperatures, while tert-butyl alcohol (TBA) exhibited a much lower performance. In situ diffuse reflectance infrared Fourier transform spectroscopy was used to clarify the remarkable influence of the alcohol structure on NO_x reduction. A high surface concentration of enolic species was observed during the partial oxidation of BA, IBA, and SBA, leading to a high concentration of isocyanate species and high NO_x conversion. However, due to the absence of α -H, it was difficult to partially oxidize TBA to form the enolic species, which resulted in its low efficiency for NO_x reduction. Based on the results obtained, a mechanism was proposed to explain the close relationship between the structure feature of alcohols and NO_x reduction efficiency.

© 2010 Elsevier Inc. All rights reserved.

1. Introduction

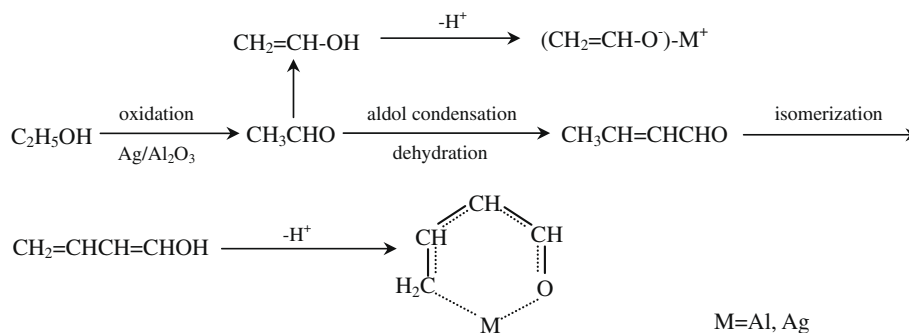
The selective catalytic reduction of NO_x by hydrocarbons (HC-SCR) has received much attention as a potential method for removing NO_x emissions from various oxygen-rich exhausts of diesel engines, lean-burn gasoline engines, and gas engines [1,2]. A number of catalysts have hitherto been found to be effective for NO_x reduction in the presence of excess oxygen, of which alumina-supported silver catalyst (Ag/Al₂O₃) is one of the most effective for the HC-SCR of NO_x [3–12]. When using oxygenated hydrocarbons, particularly ethanol as a reductant, Ag/Al₂O₃ shows high activity even in the presence of SO₂ and H₂O [3]. To improve the overall performance of Ag/Al₂O₃ for NO_x reduction, much effort has been devoted to gaining insight into the reaction mechanism. Generally, the SCR of NO_x by ethanol can be considered as follows: $\text{NO} + \text{O}_2 + \text{C}_2\text{H}_5\text{OH} \rightarrow \text{NO}_x$ (adsorbed nitrate in particular) + $\text{ad-C}_x\text{H}_y\text{O}_z \rightarrow \text{R-ONO} + \text{R-NO}_2 \rightarrow \text{-NCO} + \text{-CN} \rightarrow \text{N}_2$ [5,6,10–15]. Nevertheless, many questions remain regarding the details of this multi-step process. It has been proposed that acetate derived from the partial oxidation of ethanol plays a crucial role in the formation of isocyanate species (-NCO), as well as in the global NO_x reduction process [9,10,12,14]. From our recent research, large amounts of surface enolic species were observed by in situ diffuse reflectance infrared Fourier transform spectroscopy (DRIFTS) during both the partial oxidation of ethanol and the NO_x reduction with

ethanol over Ag/Al₂O₃. The surface enolic species exhibited much higher activity in reaction with nitrate and/or $\text{NO} + \text{O}_2$ to form -NCO species than that of acetate, demonstrating its crucial role in the SCR of NO_x by ethanol [16–20]. Previous research has identified that the enolic species also plays a key role in NO_x reduction by other alcohols (isopropyl alcohol, 1-propanol, 1-butanol) over Ag/Al₂O₃ [20–22], acetaldehyde over Ag/Al₂O₃ [16] and Co/Al₂O₃ [23], and acetylene over ZSM-5 [24]. Interestingly, substantial quantities of enols in the gas phase have been observed by photoionization mass spectrometry during hydrocarbon combustion [25] and catalytic oxidation [26]. The above results strongly suggest that adsorbed enolic species and/or enols in the gas phase are common intermediates involved in the partial oxidation chemistry of hydrocarbons and oxygenated hydrocarbons. During NO_x reduction by ethanol over Ag/Al₂O₃, it has been proposed that ethanol principally reacts with oxygen to form acetaldehyde, which is followed by isomerization to ethenol. Additionally, an enolic anion ($\text{CH}_2=\text{CH-O}^-$)– M^+ is formed by hydrogen extraction when ethenol is adsorbed on the surface of Ag/Al₂O₃. Meanwhile, the possible occurrence of aldol condensation of acetaldehyde may lead to the formation of C₄ enolic species as shown in Scheme 1 [18].

Obviously, if the formation of surface enolic species follows the hypothesis as described above, two prerequisites must be met. Firstly, the selected reductant must contain at least one C–C bond. This has been clarified by our previous research, in which the enolic species was rarely observed when CH₃OH and CH₃OCH₃ were partially oxidized over Ag/Al₂O₃ [21,22]. Secondly, it is widely accepted that the structure feature of H–C–O–H is required for

^{*} Corresponding author. Fax: +86 10 6284 9123.

E-mail address: honghe@rcees.ac.cn (H. He).



Scheme 1. The hypothesis for the surface enolic species formation during the partial oxidation of ethanol on Ag/Al₂O₃.

the partial oxidation of alcohols to aldehydes and/or ketones. That is, the OH group must be attached to a carbon atom that is bonded to at least one hydrogen atom (denoted as α -H). Considering that enols are the tautomers of aldehyde/ketones, the presence of α -H is also a prerequisite for the formation of enolic species during partial oxidation of alcohols over Ag/Al₂O₃. To highlight this issue in the present study, butyl alcohol isomers with and without α -H were employed as reductants for the NO_x reduction over Ag/Al₂O₃. Through the combination of the DRIFTS results and the activity measurements, the crucial role of surface enolic species in the SCR of NO_x by alcohols was further identified, which also provides an intrinsic criterion for the selection of reductants with high efficiency for NO_x removal.

2. Experimental

2.1. Catalyst preparation

The 4 wt.% Ag/Al₂O₃ catalyst was prepared by impregnation of pseudoboehmite powder (AlOOH, 292 m² g⁻¹) with an appropriate amount of silver nitrate aqueous solution and was then evaporated to dryness in a rotary evaporator at 333 K under reduced pressure. The resulting paste was dried at 393 K overnight and then calcined in air at 873 K for three hrs. Before the catalytic activity test, the catalyst was sieved through 20–40 meshes.

2.2. Catalytic activity test

The catalytic activity was measured with a fixed-bed quartz flow reactor (inner diameter 10 mm) by passing a mixture of 800 ppm NO, 783 ppm butyl alcohol isomers (BA, IBA, SBA or TBA), 10 vol.% H₂O, and 10 vol.% O₂ in N₂ at a rate of 2000 ml min⁻¹ over 0.6 g catalyst ($W/F = 0.018$ g s ml, $GHSV = \sim 50,000$ h⁻¹). An aqueous solution of C4 alcohol was supplied with a syringe pump into the gas stream and vaporized by a coiled heater at the inlet of the reactor. NO_x conversion was analyzed online by a chemiluminescence NO/NO₂/NO_x analyzer (42C-HL, Thermo Environmental). Analysis of the concentrations of by-products such as N₂O, NH₃, and organo-nitrogen compounds (R-ONO, R-NO₂) was carried out using an online Nicolet 380-FT-IR spectrophotometer (Thermo Nicolet) equipped with a gas cell of volume 0.2 dm³. In this case, the gas cell of 380-FT-IR spectrophotometer and gas line after the reactor were heated to 120 °C to avoid water condensation.

2.3. In situ DRIFTS studies

In situ DRIFTS spectra were recorded on a Nexus 670 FT-IR spectrophotometer (Thermo Nicolet), equipped with an in situ diffuse reflection chamber and a high-sensitivity MCT detector cooled by liquid nitrogen. The Ag/Al₂O₃ catalyst used in the in situ DRIFTS

studies was finely ground and placed into a ceramic crucible in the in situ chamber. Mass flow controllers and a sample temperature controller were used to simulate the real reaction conditions. Prior to recording each DRIFTS spectrum, the Ag/Al₂O₃ catalyst was heated in situ in a flow of O₂ + N₂ for 60 min at 873 K, then cooled to the desired temperatures for taking the reference spectrum. Water vapor was introduced into the gas stream by means of a syringe pump and carried into the in situ DRIFTS chamber. Water vapor in the gas phase and adsorbed water molecules on the surface of Ag/Al₂O₃ show strong infrared adsorption, so a reference spectrum of Ag/Al₂O₃ in a flow of O₂ + N₂ (and water vapor, where appropriate) was subtracted from each spectrum at the respective temperature. All gas mixtures were fed at a flow of 300 ml min⁻¹. All spectra reported here were taken at a resolution of 4 cm⁻¹ for 32 scans.

3. Results

3.1. Catalytic activity of Ag/Al₂O₃ for NO_x reduction by butyl alcohol isomers

The results obtained for the catalytic activities of Ag/Al₂O₃ for the SCR of NO_x by butyl alcohol isomers are shown in Fig. 1. When using TBA as a reductant, NO_x conversion was below 23%, even at temperatures of up to 673 K. After this, however, the NO_x conversion increased rapidly as temperatures increased and reached a

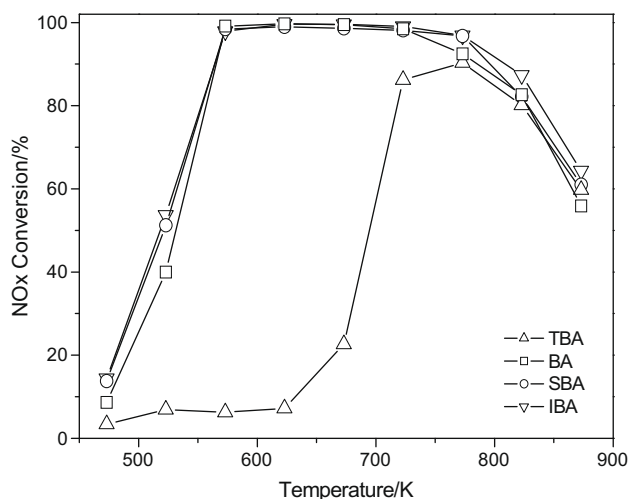


Fig. 1. Activities of 4 wt.% Ag/Al₂O₃ for the SCR of NO_x with various reductants. Reaction conditions: NO 800 ppm, TBA, BA, SBA or IBA 783 ppm, O₂ 10 vol.%, H₂O 10 vol.%, N₂ as balance; total flow = 2000 ml min⁻¹, $W/F = 0.018$ g s ml, $GHSV = \sim 50,000$ h⁻¹.

maximum of 90% at 773 K. As for BA, however, the Ag/Al₂O₃ showed much higher efficiency for NO_x reduction, particularly in the low temperature range. The NO_x conversion started at 473 K and rapidly increased to 40% with a temperature increase to 523 K. The maximum NO_x conversion reached 99% at 673 K, and the average NO_x conversion was 90%, even within the wide temperature range of 573–773 K. In the case of NO_x reduction by IBA and SBA, very similar NO_x conversions were obtained within the temperature range of 473–873 K compared with that of BA. These results suggest that NO_x reduction by BA, IBA, and SBA possibly follows similar reaction pathways, while NO_x conversion by TBA may undergo a different reaction mechanism.

During this process, the formation of by-products (N₂O, NH₃, and organo-nitrogen compounds) was measured online by a Nicolet 380-FT-IR spectrophotometer. When using TBA as a reductant, the maximum concentration of N₂O was 3.0 ppm (823 K). As for BA, SBA, and IBA, the maximum value of N₂O was 11.1 (573 K), 8.1 (573 K), and 11.2 ppm (523 K), respectively. In all cases, only trace amount of organo-nitrogen compounds was observed, suggesting that Ag/Al₂O₃ possesses high selectivity to N₂ during the NO_x reduction by butyl alcohol isomers.

3.2. In situ DRIFTS study

3.2.1. Steady state in situ DRIFTS study of the partial oxidation of C₄ alcohols

Considering that the HC-SCR of NO_x starts with the partial oxidation of the reductant, the in situ DRIFTS spectra observed during partial oxidation of butyl alcohol isomers over Ag/Al₂O₃ were first

investigated. The in situ DRIFTS of Ag/Al₂O₃ spectra in flowing TBA + O₂ at different temperatures are shown in Fig. 2. At 523 K, the feature peaks of adsorbed TBA over Ag/Al₂O₃ were clearly observed according to the intensive study of Korppi-Tommola [27]. Peaks at 1470, 1389, and 1365 cm⁻¹ were attributed to methyl bending of tert-butyl. Peaks at 1232 and 1205 cm⁻¹ were assigned to skeletal stretching of tert-butyl. The OH bending frequency was rarely observed, indicating that adsorbed TBA may present as tert-butyl ester. Meanwhile, a small amount of formate was observed at 1593 and 1392 cm⁻¹, which can be assigned to the asymmetric and symmetric stretching vibration modes of carboxyl (COO), respectively [28,29]. The further increase of the temperature to 623 K resulted in the formation of large amounts of formate at the expense of a sharp decrease in the intensities of adsorbed TBA peaks. Within the high temperature range of 673–773 K, strong peaks were observed at 1578 and 1462 cm⁻¹, indicating the formation of a large amount of acetate [30,31]. Based on our previous studies [16–22], the shoulder at 1633 cm⁻¹ can be assigned to the asymmetric stretching vibration mode of C=C–O⁻, as the structure feature of surface enolic species. Our previous research also suggests that for the enolic species, there should be other two peaks at around 1416 and 1336 cm⁻¹, attributed to the symmetric stretching vibration of C=C–O⁻ and C–H deformation mode, respectively. The absence of the two peaks, however, could be due to the low concentration of the enolic species over Ag/Al₂O₃ during the SCR of NO_x by TBA. The appearance of formate and acetate species indicated that chemical bond breakage of TBA and further oxidation occurred.

The same set of experiments was performed after exposing the catalyst to BA + O₂, with the results shown in Fig. 2B. At 523 K, a

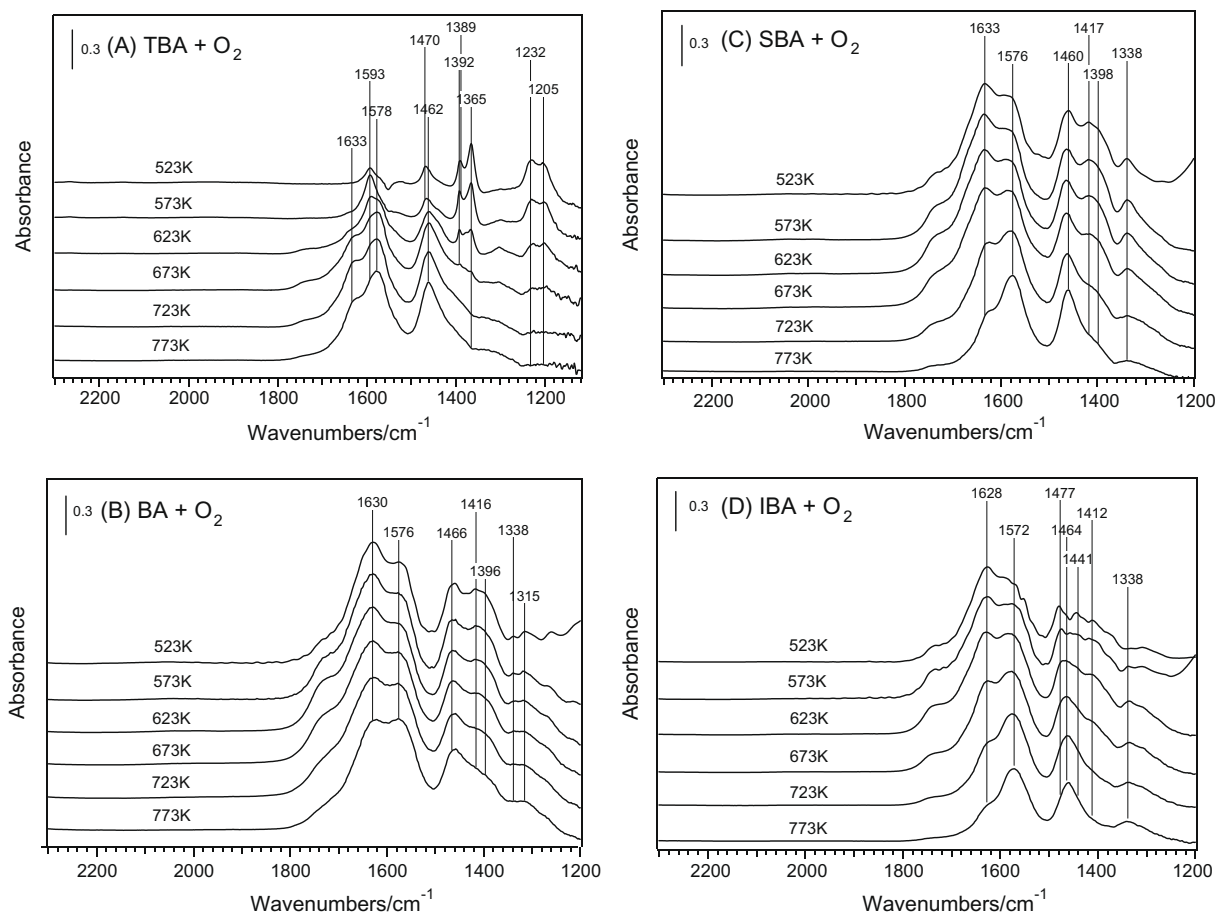


Fig. 2. In situ DRIFTS spectra of the adsorbed species over Ag/Al₂O₃ in a steady state at different temperatures during the partial oxidation of (A) TBA, (B) BA, (C) SBA, and (D) IBA. Reaction conditions: TBA, BA, SBA, or IBA 783 ppm, O₂ 10 vol.%, H₂O 10 vol.%, N₂ as balance; total flow = 300 ml min⁻¹.

strong peak was observed at 1630 cm^{-1} , together with peaks at 1416 and 1338 cm^{-1} , which can be attributed to surface enolic species [16–22]. Meanwhile, surface acetate was observed at 1576 and 1466 cm^{-1} . Increasing the temperature to 573 K enhanced the formation of enolic species, and within the wide temperature range of 523 – 723 K , the peak at 1630 cm^{-1} showed the strongest intensity, indicating that the enolic species was dominant during this process. A further increase in the temperature to 773 K decreased the intensity of the enolic species and acetate became dominant on the surface of $\text{Ag}/\text{Al}_2\text{O}_3$.

The in situ DRIFTS spectra of $\text{Ag}/\text{Al}_2\text{O}_3$ observed during the partial oxidation of SBA are shown in Fig. 2C. The enolic species was observed at 1633 , 1417 , and 1338 cm^{-1} , and this species was dominant within the temperature range of 523 – 673 K . Increasing the temperature to 723 and 773 K enhanced the conversion of enolic species to acetate (1576 and 1460 cm^{-1}). In addition, the observed peak at 1398 cm^{-1} was attributed to methyl bending. Compared to the partial oxidation of SBA, very similar DRIFTS spectra were obtained when $\text{Ag}/\text{Al}_2\text{O}_3$ was exposed to IBA in the presence of excess oxygen within the temperature of 523 – 773 K (Fig. 2D).

3.2.2. Dynamic study of the reactivity of the surface adsorbed species over $\text{Ag}/\text{Al}_2\text{O}_3$

The reactivity of the partial oxidation products of butyl alcohol isomers was further investigated by the transient response of in situ DRIFTS method. First, we chose the temperature of 723 K for TBA and 573 K for the other three alcohols as the examined temperature at which $\text{Ag}/\text{Al}_2\text{O}_3$ gave moderate NO_x conversions and high concentrations of partial oxidation products. After the catalyst was exposed to $\text{TBA} + \text{O}_2$ for 60 min at 723 K (Fig. 3A),

strong peaks appeared, attributed to the acetate species at 1578 and 1458 cm^{-1} , together with a shoulder of the enolic species at 1632 cm^{-1} . In order to clearly observe the dynamic changes of surface species mentioned above, the spectra in the range of 1200 – 2500 cm^{-1} were fitted on the basis of the deconvoluted curves. The integrated areas of the peaks at 1458 , 1632 , and 2229 cm^{-1} in Fig. 3A are displayed as a function of time on stream in Fig. 3B. Switching the feed gas to $\text{NO} + \text{O}_2$ resulted in a sharp decrease in the intensity of enolic species and acetate. A new peak of $-\text{NCO}$ appeared at 2229 cm^{-1} [5,6,9,32–36], and its intensity increased with time on stream, reaching a maximum at 3 min and then decreasing gradually. After the flowing of $\text{NO} + \text{O}_2$ for 10 min , the enolic species decreased slowly and the intensity of the $-\text{NCO}$ peak significantly decreased. Although the intensity of the acetate species consistently decreased over the remaining time, $-\text{NCO}$ showed a very low concentration, indicating that acetate is not highly reactive toward $\text{NO} + \text{O}_2$ forming $-\text{NCO}$. In addition, the appearance of peaks at 1302 and 1252 cm^{-1} indicates the formation of surface nitrate species [6,9,10,17].

The reactivity of the partial oxidation products of BA was studied in a flow of $\text{NO} + \text{O}_2$ at 573 K , and the results are exhibited in Fig. 3C and D. After exposing $\text{Ag}/\text{Al}_2\text{O}_3$ to $\text{BA} + \text{O}_2$ for 60 min , large amounts of enolic species (1633 , 1412 , and 1340 cm^{-1}) and acetate (1578 and 1466 cm^{-1}) were observed, and the former was dominant. When switching the feed gas to $\text{NO} + \text{O}_2$, the peak at 2243 cm^{-1} attributed to $-\text{NCO}$ appeared at 2 min . As the enolic species decreased gradually, a large amount of $-\text{NCO}$ species was formed and remained at high concentrations even after 60 min . After purging $\text{NO} + \text{O}_2$ for 60 min , the intensity of acetate species did not decrease but increased slightly, indicating that the enolic

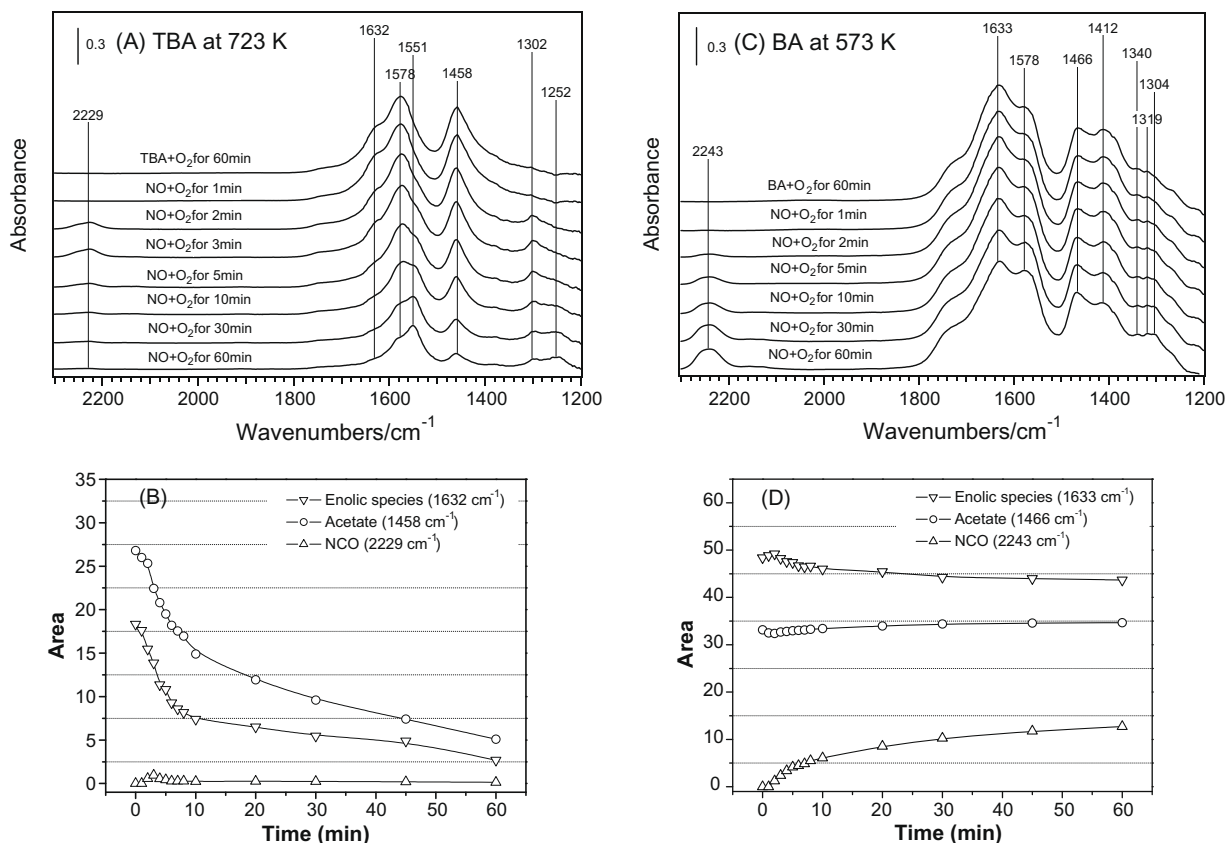


Fig. 3. Dynamic changes of in situ DRIFTS spectra of $\text{Ag}/\text{Al}_2\text{O}_3$ as a function of time in a flow of NO (800 ppm) + O_2 ($10\text{ vol.}\%$) at a constant temperature after exposing to (A) $\text{TBA} + \text{O}_2$ at 723 K , (C) $\text{BA} + \text{O}_2$, (E) $\text{SBA} + \text{O}_2$, (G) $\text{IBA} + \text{O}_2$ at 573 K for 60 min in the presence of $10\text{ vol.}\%$ H_2O . (B), (D), (F), and (H): time dependence of the integrated areas of the peaks of $-\text{NCO}$ (Δ), enolic species (∇), and acetate (\circ) for the case of (A), (C), (E), and (G), respectively.

species can further oxidize to produce acetate. These results strongly suggest the enolic species possess higher activity for reaction with $\text{NO} + \text{O}_2$ to form $-\text{NCO}$ than that of acetate, which was in good agreement with our previous work [16,17,21].

The reactivity of the partial oxidation products of SBA and IBA was evaluated in essentially the same manner as that of BA, and similar changes were observed (Fig. 3E–H). In both cases, the enolic species and acetate were the main products, with the former being dominant after partial oxidation of SBA and IBA over $\text{Ag}/\text{Al}_2\text{O}_3$. The concentration of enolic species decreased gradually, whereas the concentration of surface acetate increased a little bit over time. During this process, large amounts of $-\text{NCO}$ were formed even after switching the feed gas to $\text{NO} + \text{O}_2$ for 60 min, further demonstrating that the enolic species reacts more efficiently with $\text{NO} + \text{O}_2$ than the acetate species to obtain high concentrations of surface $-\text{NCO}$.

To further investigate the reactivity of enolic species, acetate and $-\text{NCO}$, the same experiments were performed at elevated temperatures of 673 and 723 K after SA partial oxidation. As shown in Fig. 4A and B, high concentrations of enolic species and acetate were formed after exposure of $\text{Ag}/\text{Al}_2\text{O}_3$ to $\text{BA} + \text{O}_2$ at 673 K. Switching the feed gas to $\text{NO} + \text{O}_2$ results in the formation of $-\text{NCO}$ at the first minute, reaching the maximum at 4 min, and then remaining at high concentrations within following 5 min. Simultaneously, a significant decrease in the intensity of enolic species was observed while the concentration of acetate decreased slowly, further demonstrating a higher reactivity of the former than the latter. The further increase of the temperature to 723 K accelerated the reaction of enolic species with $\text{NO} + \text{O}_2$ to form $-\text{NCO}$ and further reaction of $-\text{NCO}$ with $\text{NO} + \text{O}_2$ to N_2 (Fig. 4C and D). A sharp decrease in the surface concentration of enolic species was observed within 3 min, and the maximum value of $-\text{NCO}$ appeared at 2 min,

which was followed by a quick decrease in the concentration. This result clearly shows that the $-\text{NCO}$ can be regarded as a key intermediate for NO_x reduction by BA, originating from the reaction between enolic species and $\text{NO} + \text{O}_2$, and possessing high reactivity toward $\text{NO} + \text{O}_2$ to form N_2 .

The reactivity of the partial oxidation products of SBA and IBA was evaluated in essentially the same manner as that of BA at 673 and 723 K. In all cases, enolic species exhibits higher activity for reaction with $\text{NO} + \text{O}_2$ to produce $-\text{NCO}$ than acetate; the $-\text{NCO}$ species as the key intermediate for NO_x reduction possesses high reactivity toward $\text{NO} + \text{O}_2$; elevated reaction temperature favors both the $-\text{NCO}$ formation and its further reaction with $\text{NO} + \text{O}_2$.

3.2.3. Steady state *in situ* DRIFTS study of the SCR of NO_x by C4 alcohols over $\text{Ag}/\text{Al}_2\text{O}_3$

To further identify the mechanisms of the SCR of NO_x by butyl alcohol isomers over $\text{Ag}/\text{Al}_2\text{O}_3$, *in situ* DRIFTS experiments were carried out in the temperature range of 473–773 K. The DRIFTS spectra of $\text{Ag}/\text{Al}_2\text{O}_3$ in a flow of TBA + $\text{NO} + \text{O}_2$ are shown in Fig. 5A. As mentioned earlier, the bands at 1392, 1365, 1234, and 1200 cm^{-1} attributable to tert-butyl ($-\text{C}(\text{CH}_3)_3$) of the adsorbed TBA species were observed at temperatures below 673 K. According to the literatures [6,9,10,17], the bands at 1537 and 1302 cm^{-1} can be attributed to adsorbed nitrate species, and the peaks at 1576 and 1462 cm^{-1} are associated with the surface acetate species. An increase in the reaction temperature results in a gradual decrease in the intensity of the peaks attributed to adsorbed TBA and leads to an increase in the intensity of the acetate peaks. Simultaneously, enolic species (1633 cm^{-1}) was observed at above 573 K, and a weak peak at 2227 cm^{-1} attributed to $-\text{NCO}$ was observed within the temperature range of 623–773 K

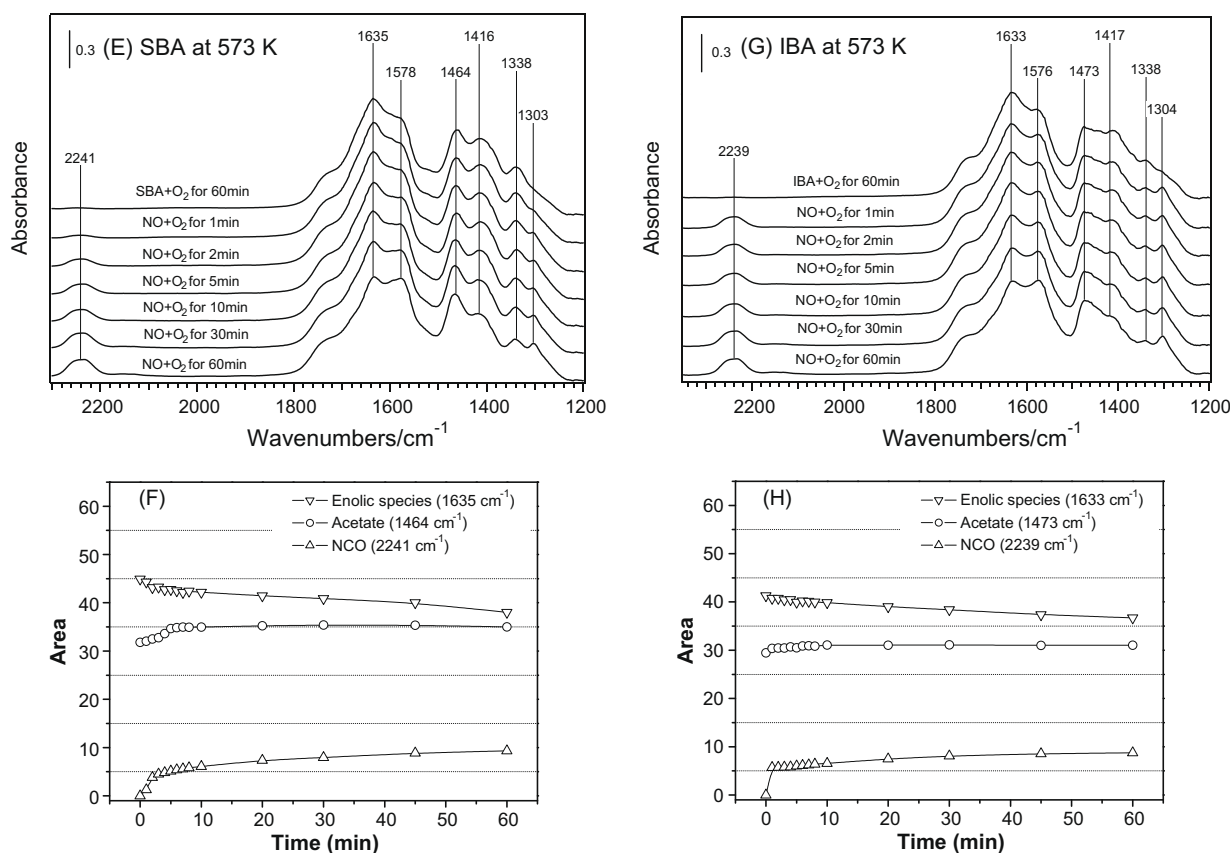


Fig. 3 (continued)

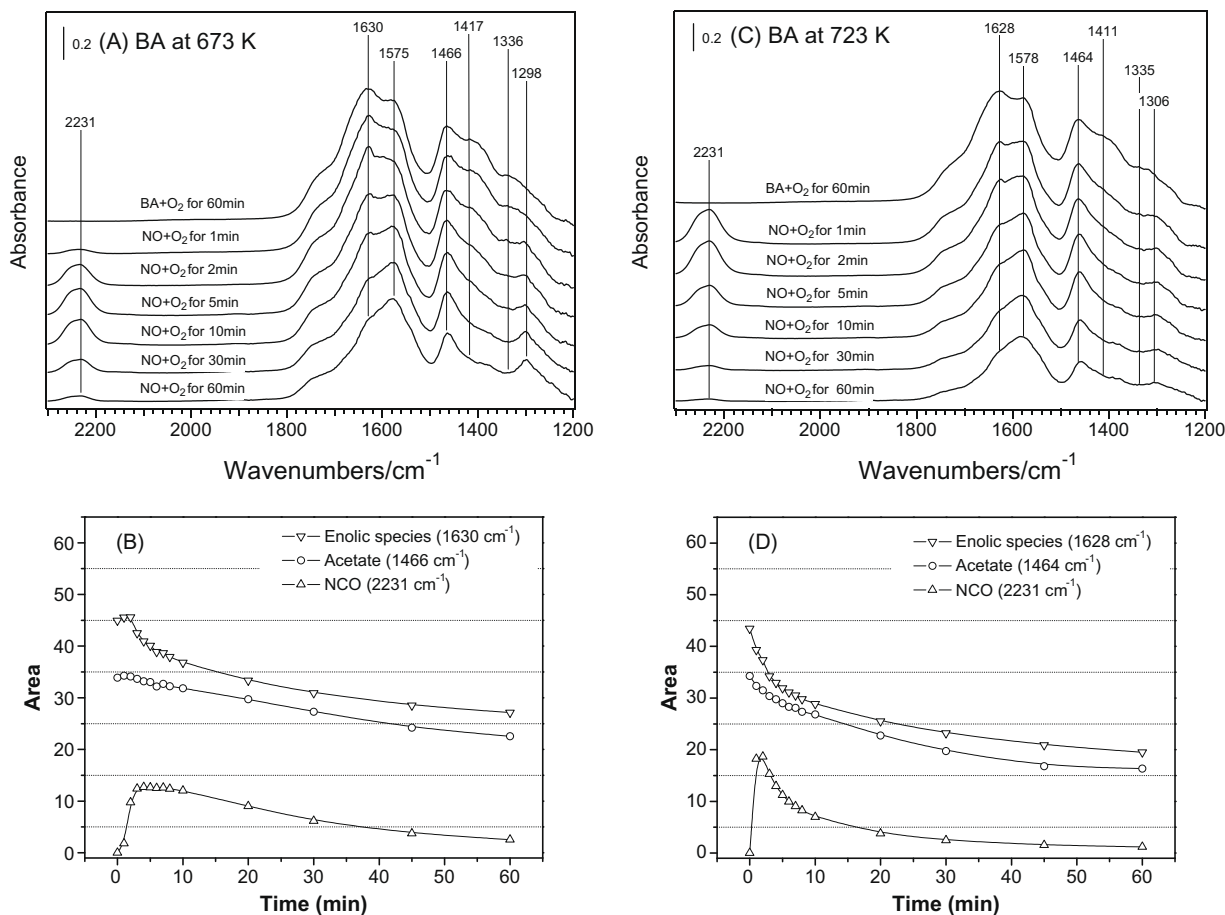


Fig. 4. Dynamic changes of in situ DRIFTS spectra of $\text{Ag}/\text{Al}_2\text{O}_3$ as a function of time in a flow of NO (800 ppm) + O_2 (10 vol.%) at a constant temperature after exposing to $\text{BA} + \text{O}_2$ at (A) 673 K and (C) 723 K for 60 min in the presence of 10 vol.% H_2O . (B) and (D): time dependence of the integrated areas of the peaks of $-\text{NCO}$ (Δ), enolic species (∇), and acetate (\circ) for the cases of (A) and (C), respectively.

[5,6,9,32–36]. The peak at 1591 cm^{-1} can be assigned to formate species.

The in situ DRIFTS spectra over $\text{Ag}/\text{Al}_2\text{O}_3$ in a flow of $\text{BA} + \text{NO} + \text{O}_2$ are shown in Fig. 5B. Strong peaks of acetate (1570 and 1466 cm^{-1}) and nitrate (1585 and 1304 cm^{-1}) were detected on the surface. Different from the case of TBA, a strong peak was observed at 1635 cm^{-1} , together with shoulders at 1412 and 1338 cm^{-1} in the temperature region of 473 – 673 K , suggesting a large amount of surface enolic species on the catalyst. As the intensity of the enolic species and nitrate decreased with increased temperature, a $-\text{NCO}$ peak at 2231 cm^{-1} appeared at 523 K and remained at high intensity within the wide temperature range of 573 – 773 K . Similar DRIFTS spectra were observed during the NO_x reduction by IBA and SBA (Fig. 5C and D), where strong enolic species (1635 – 1637 , 1415 – 1417 , and 1338 cm^{-1}), acetate species (1572 – 1576 , 1462 – 1464 cm^{-1}), and nitrate species (1589 – 1593 , 1556 , and 1302 cm^{-1}) were also observed. The enolic species was also dominant within moderate temperatures, and there was a large amount of $-\text{NCO}$ at temperatures above 523 K on the $\text{Ag}/\text{Al}_2\text{O}_3$ surface. In both cases, peaks due to methyl bending were observed at 1392 and 1379 cm^{-1} .

4. Discussion

As shown in Fig. 1, BA, SBA, and IBA possess similar high efficiency for NO_x reduction over $\text{Ag}/\text{Al}_2\text{O}_3$, providing a 50% NO_x conversion (T_{50}) at 531 , 520 , and 518 K , respectively. However, NO_x

reduction by TBA over $\text{Ag}/\text{Al}_2\text{O}_3$ exhibits a much lower NO_x conversion in the temperature range of 473 – 723 K , providing a T_{50} for NO_x conversion at around 694 K , which is about 176 K higher than that of the T_{50} by IBA.

It has been widely accepted that $-\text{NCO}$ species is the key intermediate in the SCR of NO_x by hydrocarbons or oxygenates over $\text{Ag}/\text{Al}_2\text{O}_3$. This species possesses high reactivity toward $\text{NO} + \text{O}_2$ to produce N_2 , and its high productivity on the catalyst surface indicates its high efficiency for NO_x reduction [32–35]. Obviously, in the case of NO_x reduction by BA, SBA, and IBA (Fig. 5), the formation of $-\text{NCO}$ always occurred at around 520 K , at which point the catalyst light-off for NO_x reduction was achieved (Fig. 1). The high surface concentration of this species was maintained within the temperature range of 573 – 773 K , which is related to its high efficiency for NO_x conversion. In relation to NO_x reduction by TBA, however, the $-\text{NCO}$ species was rarely observed, even at temperatures as high as 623 K (Fig. 5), which results in low NO_x conversion by TBA. The results clearly indicate that the different surface concentrations of $-\text{NCO}$ in the cases of using TBA or the other three butyl alcohol isomers as reductants caused the differences in NO_x reduction activity.

It has also been widely accepted that the partial oxidation of reductant plays a crucial role in the formation of $-\text{NCO}$ during the HC-SCR of NO_x [6,9–15,30,31]. From the in situ DRIFTS spectra of partial oxidation of BA, SBA, and IBA, the enolic species was shown to be predominant within the low temperature range of 523 – 673 K , together with the formation of large amounts of acetate. The enolic species showed higher activity toward $\text{NO} + \text{O}_2$ to

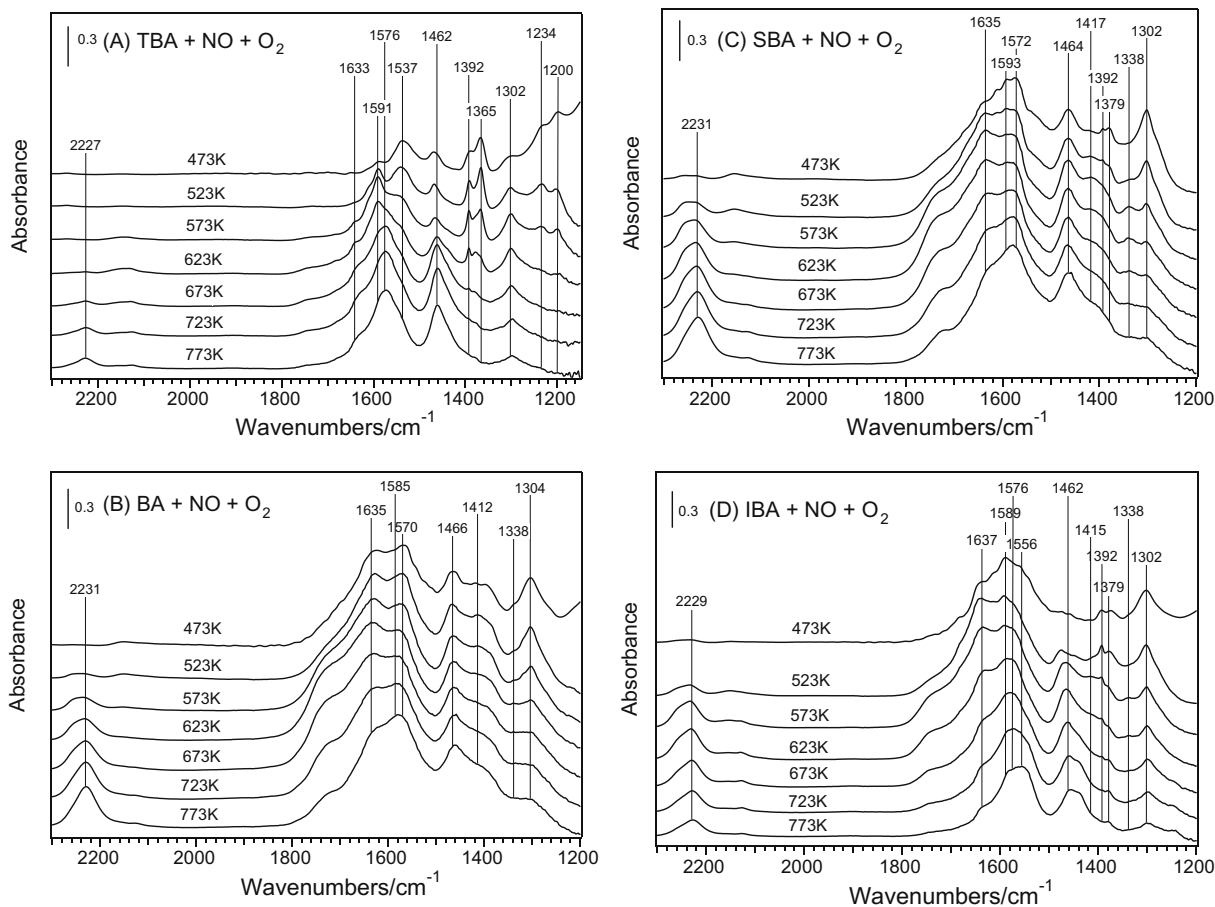
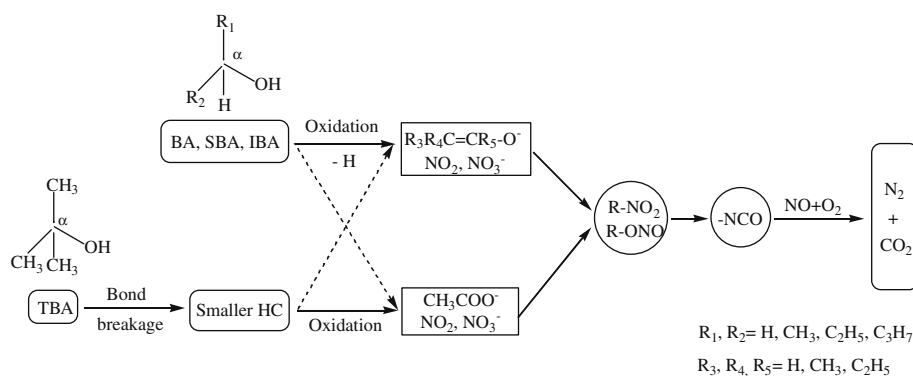


Fig. 5. In situ DRIFTS spectra of the absorbed species over Ag/Al₂O₃ in a steady state at different temperatures during the SCR of NO_x by (A) TBA, (B) BA, (C) SBA, and (D) IBA. Reaction conditions: NO 800 ppm, TBA, BA, SBA, or IBA 783 ppm, O₂ 10 vol.%, H₂O 10 vol.%, N₂ as balance; total flow = 300 ml min⁻¹.



Scheme 2. The proposed mechanism of the SCR of NO_x by butyl alcohol isomers over Ag/Al₂O₃.

form -NCO than acetate and resulted in a high surface concentration of -NCO species (Figs. 3 and 4). This relates to the high efficiency of NO_x reduction by these three alcohols. In relation to TBA, however, the partial oxidation at temperatures below 573 K is difficult. Consequently, it is reasonable that TBA shows lower NO_x conversion at this temperature range. At temperatures above 573 K, acetate, not enolic species, became the main surface species. In this case, the acetate plays a key role in -NCO formation and results in a lower concentration of -NCO during the NO_x reduction by TBA over Ag/Al₂O₃.

After exposing the catalyst to BA + O₂ for 60 min at 573 K (Fig. 3C and D), the surface was covered by high concentration of

enolic species and acetate. With this in mind, the monotonic increase in integral intensity of -NCO during flowing NO + O₂ at 573 K possibly caused by the insufficiency of active sites available for NO oxidation and nitrate formation. Elevated the reaction temperatures decreased the surface concentration of enolic species, providing more active sites for NO oxidation and nitrate formation, hence accelerating the consumption of -NCO by NO + O₂ to produce N₂, with the results shown in Fig. 4B and D.

As reported by Sachtler and coworkers [37,38], there is another route leading to N₂ formation via isocyanate hydrolysis during the HC-SCR of NO_x. In this case, -NCO is to be hydrolyzed by water to produce more reactive ammonia to form N₂ over zeolite-based cat-

alysts. As suggested by Haneda et al. [39], —NCO was hydrolyzed to the surface —NH complexes by the reaction with traces of water during NO_x reduction by propene over $\text{Ga}_2\text{O}_3\text{—Al}_2\text{O}_3$, giving the N—H stretching vibration at around 3400 cm^{-1} . In our case, however, the N—H stretching vibration was hardly observed, indicating that the pathway involved in the hydrolyzation of —NCO could be neglectable in the SCR of NO_x by C4 alcohols over $\text{Ag/Al}_2\text{O}_3$.

It is obvious now that different structures of butyl alcohol isomers result in different surface concentrations of the partial oxidation products and different concentrations of —NCO , which subsequently contributes to the different performances of $\text{Ag/Al}_2\text{O}_3$ for NO_x reduction by these alcohols.

In essence, the partial oxidation of alcohols to aldehydes and/or ketones can be regarded as a dehydrogenation reaction, suggesting that the structural feature of H—C—O—H is required for this process. In other words, the OH group must be attached to a carbon atom that is bonded to at least one $\alpha\text{-H}$. It is clear that tertiary alcohols such as TBA cannot undergo oxidation to form aldehydes and/or ketones because of the absence of $\alpha\text{-H}$. Since enols in the gas phase and adsorbed enolic species are the tautomers of aldehydes and ketones, the presence of $\alpha\text{-H}$ is also a prerequisite for their formation during the partial oxidation of alcohols over $\text{Ag/Al}_2\text{O}_3$. As a result, large amounts of enolic species were formed during the partial oxidation of IB, SBA, and IBA over $\text{Ag/Al}_2\text{O}_3$ at low temperatures. In addition, these three alcohols and/or enolic species can be broken up into smaller hydrocarbon molecules, which are subsequently oxidized to acetate, particularly in high temperatures. In relation to TBA, the elimination of $\alpha\text{-H}$ is impossible and thus the partial oxidation follows a different pathway. Its oxidation process starts with the breakup of the carbon chain into smaller molecules, which requires extra energy and therefore tends to favor high temperatures. Results from this study show that at high temperatures, oxidation of the smaller molecules to acetate and formate occurred, together with the formation of trace amounts of surface enolic species.

On the basis of the above analyses, together with the results of previous studies [5,6,10–20], the mechanisms of the SCR of NO_x by C4 alcohols with different structures were proposed in Scheme 2. The reaction starts with the formation of both adsorbed nitrates via NO oxidation by O_2 and enolic species and acetate via the partial oxidation of alcohols over $\text{Ag/Al}_2\text{O}_3$. The reaction between the two kinds of adsorbed species then leads to the formation of —NCO , possibly via organo-nitrogen compounds (such as R—ONO and R—NO_2). Subsequently, —NCO reacts with $\text{NO} + \text{O}_2$ and/or nitrates to yield N_2 . The enolic species and surface acetate, as the intermediates derived from the partial oxidation of reductants, show different activity to form —NCO . TBA follows the pathway involved in the breakup of the carbon chain and then oxidation to acetate and formate. The relatively low activity of acetate and formate toward $\text{NO} + \text{O}_2$ results in a low concentration of —NCO [17,21,22], finally relating to a low NO_x conversion by TBA. In regard to NO_x reduction by primary and secondary butyl alcohols (BA, SBA and IBA), however, the presence of $\alpha\text{-H}$ opens an avenue to the formation of enolic species. Its high surface concentration and high reactivity toward $\text{NO} + \text{O}_2$ results in high concentrations of —NCO , which determines the high efficiency for NO_x reduction by these three alcohols over $\text{Ag/Al}_2\text{O}_3$.

5. Conclusions

Alcohol structure has a significant influence on the activity of $\text{Ag/Al}_2\text{O}_3$ for NO_x reduction by butyl alcohol isomers, including

TBA, BA, SBA, and IBA. Similarly high activity for NO_x reduction over $\text{Ag/Al}_2\text{O}_3$ was shown for BA, IBA, and SBA, while TBA gave a much lower NO_x conversion in the temperature range of 473–773 K. BA, IBA, and SBA containing $\alpha\text{-H}$ are favorable for the partial oxidation to form enolic species, while the $\alpha\text{-H}$ participated reaction pathway is impossible for TBA due to the absence of $\alpha\text{-H}$. The dominant pathway of TBA oxidation involves the breakup of alcohol molecules, leading to an oxidation to acetate and formate. The lower reactivity of the acetate and formate toward NO_x resulted in a low concentration of —NCO species, and consequently low NO_x conversion. Our study provides an intrinsic criterion for the selection of alcohols as reductants with high efficiency for NO_x removal.

Acknowledgments

This work was financially supported by the National Natural Science Foundation of China (20773158, 50921064) and the Knowledge Innovation Program of the Chinese Academy of Sciences (KZCX1-YW-06-04).

References

- [1] M. Iwamoto, H. Yahiro, *Catal. Today* 22 (1994) 5.
- [2] M. Shelef, *Chem. Rev.* 95 (1995) 209.
- [3] T. Miyadera, *Appl. Catal. B* 2 (1993) 199.
- [4] K.A. Bethke, H.H. Kung, *J. Catal.* 172 (1997) 93.
- [5] S. Sumiya, H. He, A. Abe, N. Takezawa, K. Yoshida, *J. Chem. Soc., Faraday Trans.* 94 (1998) 2217.
- [6] S. Kameoka, Y. Ukisu, T. Miyadera, *Phys. Chem. Chem. Phys.* 2 (2000) 367.
- [7] K. Shimizu, A. Satsuma, T. Hattori, *Appl. Catal. B* 25 (2000) 239.
- [8] A. Martínez-Ariza, M. Fernández-García, A. Iglesias-Juez, J.A. Anderson, J.C. Conesa, J. Soria, *Appl. Catal. B* 28 (2000) 29.
- [9] R. Burch, J.P. Breen, F.C. Meunier, *Appl. Catal. B* 39 (2002) 283.
- [10] Y.H. Yeom, M. Li, M.H.W. Sachtler, E. Weitz, *J. Catal.* 238 (2006) 100.
- [11] J.H. Lee, S.J. Schmieg, S.H. Oh, *Appl. Catal. A* 342 (2008) 78.
- [12] Y.F. Tham, J.-Y. Chen, R.W. Dibble, *Proc. Combust. Inst.* 32 (2009) 2827.
- [13] T. Chafik, S. Kameoka, Y. Ukisu, T. Miyadera, *J. Mol. Catal. A* 136 (1998) 203.
- [14] Y.H. Yeom, M. Li, M.H.W. Sachtler, E. Weitz, *J. Catal.* 246 (2007) 413.
- [15] R. da Silva, R. Cataluña, A. Martínez-Ariza, *Catal. Today* 143 (2009) 211.
- [16] Y. Yu, H. He, Q. Feng, *J. Phys. Chem. B* 107 (2003) 13090.
- [17] Y. Yu, H. He, Q. Feng, H. Gao, X. Yang, *Appl. Catal. B* 49 (2004) 159.
- [18] Y. Yu, H. Gao, H. He, *Catal. Today* 93–95 (2004) 805.
- [19] H. He, Y. Yu, *Catal. Today* 100 (2005) 37.
- [20] H. He, X. Zhang, Q. Wu, C. Zhang, Y. Yu, *Catal. Surv. Asia* 12 (2008) 38.
- [21] Q. Wu, H. He, Y. Yu, *Appl. Catal. B* 61 (2005) 107.
- [22] Q. Wu, Y. Yu, H. He, *Chin. J. Catal.* 27 (2006) 993.
- [23] A. Takahashi, M. Haneda, T. Fujitani, H. Hamada, *J. Mol. Catal. A* 261 (2007) 6.
- [24] Q. Yu, X. Wang, N. Xing, H. Yang, S. Zhang, *J. Catal.* 245 (2007) 124.
- [25] C.A. Taatjes, N. Hansen, A. McIlroy, J.A. Miller, J.P. Senosiain, S.J. Klippenstein, F. Qi, L. Sheng, Y. Zhang, T.A. Cool, J. Wang, P.R. Westmoreland, M.E. Law, T. Kasper, K. Kohse-Höinghaus, *Science* 308 (2005) 1887.
- [26] Y. Li, X. Zhang, H. He, Y. Yu, T. Yuan, Z. Tian, J. Wang, Y. Li, *Appl. Catal. B* 89 (2009) 659.
- [27] J. Korppi-Tommola, *Spectrochim. Acta* 34A (1978) 1077.
- [28] J. Raskó, T. Kecskés, J. Kiss, *J. Catal.* 224 (2004) 261.
- [29] C. Zhang, H. He, K. Tanaka, *Appl. Catal. B* 65 (2006) 37.
- [30] K. Shimizu, H. Kawabata, A. Satsuma, T. Hattori, *Appl. Catal. B* 19 (1998) L87.
- [31] K. Shimizu, H. Kawabata, A. Satsuma, T. Hattori, *J. Phys. Chem. B* 103 (1999) 5240.
- [32] S. Kameoka, T. Chafik, Y. Ukisu, T. Miyadera, *Catal. Lett.* 51 (1998) 11.
- [33] S. Kameoka, T. Chafik, Y. Ukisu, T. Miyadera, *Catal. Lett.* 55 (1998) 211.
- [34] N. Bion, J. Saussey, M. Haneda, M. Daturi, *J. Catal.* 217 (2003) 47.
- [35] S. Tamm, H.H. Ingelsten, A.E.C. Palmqvist, *J. Catal.* 255 (2008) 304.
- [36] F. Thibault-Starzyk, E. Seguin, S. Thomas, M. Daturi, H. Arnolds, D.A. King, *Science* 324 (2009) 1048.
- [37] H.-Y. Chen, Q. Sun, B. Wen, Y.-H. Yeom, E. Weitz, W.M.H. Sachtler, *Catal. Today* 96 (2004) 1.
- [38] B. Wen, Y.-H. Yeom, E. Weitz, W.M.H. Sachtler, *Appl. Catal. B* 48 (2004) 125.
- [39] M. Haneda, N. Bion, M. Daturi, J. Saussey, J.-C. Lavalley, D. Duprez, H. Hamada, *J. Catal.* 206 (2002) 114.